*eXPRESS Polymer Letters Vol.6, No.2 (2012) 120–128*
*Available online at www.expresspolymlett.com*
*DOI: 10.3144/expresspolymlett.2012.13*

# A detailed study of α-relaxation in epoxy/carbon nanoparticles composites using computational analysis

*A. Z. Stimoniaris*[1], *C. A. Stergiou*[2*], *C. G. Delides*[1]

[1]Technological Research Center and Technological Education Institute of Western Macedonia, Laboratories of Physics and Materials Technology, 50100 Kila, Kozani, Greece
[2]Laboratory of Materials for Electrotechnics, Department of Electrical and Computer Engineering, Aristotle University, Thessaloniki 54124 Greece

*Received 7 June 2011; accepted in revised form 7 September 2011*

**Abstract.** Nanocomposites were fabricated based on diglycidyl ether of bisphenol A (DGEBA), cured with triethylenetetramine (TETA) and filled with: a) high conductivity carbon black (CB) and b) amino-functionalized multiwalled carbon nanotubes (MWCNTs). The full dynamic mechanical analysis (DMA) spectra, obtained for the thermomechanical characterization of the partially cured DGEBA/TETA/CB and water saturated DGEBA/TETA/MWCNT composites, reveal a complex behaviour as the α-relaxation appears to consist of more than one individual peaks. By employing some basic calculations along with an optimization procedure, which utilizes the pseudo-Voigt profile function, the experimental data have been successfully analyzed. In fact, additional values of sub-glass transition temperature ($T_i$) corresponding to sub-relaxation mechanisms were introduced besides the dominant process. Thus, the physical sense of multiple networks in the composites is investigated and the glass transition temperature $T_g$ is more precisely determined, as the DMA α-relaxation peaks can be reconstructed by the accumulation of individual peaks. Additionally, a novel term, the index of the network homogeneity (*IH*), is proposed to effectively characterize the degree of statistical perfection of the network.

***Keywords:*** *nanocomposites, carbon black, carbon nanotubes, thermomechanical properties, α-relaxation analysis*

## 1. Introduction

Carbon nanoparticles (e.g. carbon black and carbon nanotubes) are widely used as a reinforcing agent in epoxy resin products to improve their mechanical, thermal and electrical properties [1, 2]. It is thus known that the addition of carbon nanoparticles into the resin matrix can dramatically change its hardness, tensile strength, elastic modulus and electrical conductivity. Specifically, the effects of the nanofillers in polymer composites on the glass transition ($T_g$) and on the relaxation behaviour of the polymer matrix have been studied for different filler–resin composites. However, the remarks on $T_g$ variation are controversial as in some cases an increase in $T_g$ with filler content is reported in the literature [3–5], yet the opposite result is possible as well [6, 7]. Additionally, the variation of $T_g$ as a function of filler content in epoxy nanocomposites shows an initial decrease up to a certain content value followed by an increase at higher filler loading [8, 9]. Therefore, the actual effect of the filler on the $T_g$ necessitates further clarification, as it is also reviewed for MWCNT composites in [10]. In general, the amount, the dispersion and the surface conditions of the nanoparticles were found to play an important role in the variation of $T_g$ and the mechanical properties of the nanocomposites [7, 11–13]. In epoxy nanocomposites and generally in thermoset nanocomposites there is an additional difficulty met, compared to the thermoplastic nano-

*Corresponding author, e-mail: stergiou.babis@gmail.com

composites. In particular, the curing conditions of the nanocomposites and their results are different from those of the pure epoxy probably due to the effect of the nanoparticles on the crosslinking mechanism [8]. With regard to the thermoset epoxies a significant amount of data has been accumulated about water absorption and diffusion and their effect on the dynamic mechanical behaviour [11, 14]. However, for the understanding and explanation of all the experimental data there are still some points open to question. Among them two different material systems, namely the sub-cured DGEBA/TETA/CB and the water-saturated DGEBA/TETA/MWCNTs composites, which exhibit complex $\tan\delta$ curves in the dynamic mechanical analysis (DMA) spectra, may function as the case studies for a more detailed analysis.

Therefore, in this work besides the study of the mechanical dynamics of epoxy nanocomposites we focus our attention on the analysis of the α-relaxation peak, where this complex relaxation spectrum appears. To this end, a computational approach is successfully applied based on the analysis of the complex $\tan\delta$ spectrum and the introduction of more than one relaxation mechanisms. In addition to the computational analysis, a new index is proposed to characterize the network homogeneity.

## 2. Experimental

### 2.1. Materials

The pre-polymer D.E.R.332 used in this study was diglycidyl ether of bisphenol A (DGEBA) supplied by Fluka SA, USA, with epoxy equivalent 190, molecular weight 380 and viscosity 15 000 cP at 25°C. The hardener used was triethylenetetramine (TETA) supplied by Sigma Aldrich, USA. The extra conductive carbon black (particle size 25–75 nm) was obtained from Degussa, Germany, whereas the multi-wall carbon nanotubes (NC3152), with average diameter of about 9.8 nm and average length of 1 μm, were supplied by Nanocyl, Belgium. All the components of the system are commercial products and they were used without further purification.

### 2.2. Sample preparation and characterization

In order to prepare the DGEBA/TETA/CB and DGEBA/TETA/MWCNT composites, the pre-polymer was initially heated at 40°C to decrease its viscosity. The necessary amounts of TETA (epoxy/TETA = 100/14) and CB or MWCNT were then added and the mixture was mechanically stirred for 1 hour at 2000 rpm and degassed under vacuum for 15 minutes. Finally, the mixture was sonicated for 30 minutes at 200 W (Hielscher ultrasonic processor), in order to suppress the possible formation of agglomerates and bundles, and degassed again. The produced homogeneous liquid was poured in rectangular shaped molds with dimensions $40 \times 10 \times 1.5$ mm and the samples were cured at 60°C for 20 hours, whereas some of the samples were subjected to an additional post-curing heat treatment at 150°C for 2 hours. For the characterization of the fabricated samples a Polymer Laboratories dynamic mechanical thermal analyzer MK III was used according to ASTM D7028-07e1. Measurements of the tensile storage and loss modulus $E'$ and $E''$ and loss tangent tanδ were performed from room temperature up to 200°C on a constant rate of 2°C/min, at the frequency of 10 Hz and with a 4% strain. In each of the tests, at least three different samples were tested, and the average results were recorded.

### 2.3. Computational approach

It is well known from polymer theory that the relaxations in polymers and especially in composites are complex processes which stem from different mechanisms [8, 11, 15–18]. Among various theoretical models, which have been proposed to describe these complex effects, the assumption that the recorded process consists of discrete elementary relaxation processes constitutes a realistic and practical approach. Therefore, we have written a specialized computer program to carry out the computational analysis of the α-relaxation in epoxy nanocomposites, where a complex behaviour appears.

Generally, the measured diagram of $y = \tan\delta$ as a function of temperature $x = T$ can be considered as the result of the contribution and overlapping of individual peaks, which correspond to distinguished relaxations and are indicative of a heterogeneous cross-link topology [19]. These phenomena can be expressed either by Gaussian (G) or Lorentzian (L) distribution, which allows the constituent curve K at the arbitrary temperature $x_i$ to be described by Equations (1) and (2):

$$\Phi_G = \frac{C_0^{1/2}}{H_K \pi^{1/2}} \exp\left( \frac{- C_0 (x_i - x_K)^2}{H_K^2} \right)$$

Gaussian (G) (1)

$$\Phi_L = \frac{C_1^{1/2}}{\pi H_K} \left( 1 + C_1 \frac{(x_i - x_K)^2}{H_K^2} \right)^{-1}$$

Lorentzian (L) (2)

where $C_0$ and $C_1$ are the normalization fitting constants, $x_K$ is the temperature at the curve's peak, and $H_K$ is the full width at half maximum (FWHM) of the curve K. Nevertheless, better results in the description of real systems can be produced by employing the pseudo-Voigt (pV) function, which is the weighted sum of both functions of Gaussian and Lorentzian formula (Equation (3)):

$$\Phi_{pV} = \eta \cdot \Phi_L + (1 - \eta) \cdot \Phi_G$$

pseudo-Voigt (pV) (3)

where $\eta \leq 1$ is the ratio between the Lorentzian and the Gaussian function. Despite the widespread use of the pV function defined in Equation (3) in materials research, for instance in X-rays diffraction and Raman spectroscopy [20, 21], to the best of our knowledge there is no previously reported application of this function in the investigation of the composites' mechanical properties.

The performed analysis constitutes a typical optimization process in pursuit of the model parameters yielding the minimum value of the selected objective functions. Specifically, as the experimental relaxation spectrum is analyzed to its constituent sub-relaxations, the objective is the minimization of the difference between the measured and calculated master curve by employing the minimum number of component K curves. The obtained characteristic parameters of each K curve are the temperature $x_K$, the value of the peak $y_K$ and the FWHM HK after the subtraction of the background. The normalization constants $C_0$ and $C_1$ for fitting the profile of functions to experimental data are also calculated by the optimization process. During the execution of the program, components can be added and their parameters can be modified. The finally calculated value yci, which corresponds to temperature $x_i$, is the sum of all contributed components $y_i = s \cdot \Phi_{pV} \cdot |x_i - x_K|$, including the background $y_b$. Therefore, $y_{ci}$ is given by Equation (4):

$$y_{ci} = s \cdot \sum_K (\Phi_{pV} \cdot |x_i - x_K|) + y_b \quad (4)$$

where the scale factor s is to be optimized as well. By using the least square method, the parameters producing the best approximation of the $y_{ci}$ calculated from the Equation (4) to the experimental values are evaluated after several iterations. By that means, the experimental profile $y = \tan\delta$ is analyzed to its constituent individual curves, serving to elucidate the complex α-relaxation spectrum of epoxy/carbon nanoparticle composites.

At this point, we should additionally define the area $S_K$ that is encompassed by one curve and the line of background, since this expresses the contribution of each mechanism to the relaxation master curve. Since the area $S_K$ of the curve K is extended to the whole temperature range of the experiment, it is given by Equation (5):

$$S_K = \sum_i \left[ \frac{1}{2} (y_i + y_{i+1})(x_{i+1} - x_i) \right] \quad (5)$$

## 3. Results and discussion

### 3.1. Theoretical background

As it is well known, the glass transition process may be considered as being controlled by the intrinsic flexibility of the backbone or as a function of the free volume available within the polymer. In the latter model, conformational change can only occur when there is sufficient free volume for the chain to move. The free volume is assumed to diffuse throughout the polymer at a rate controlled by the motion of the chains and has a critical value for the onset of large segmental motion. Moreover, according to the intrinsic flexibility approach the variation of chemical structure also involves an intermolecular contribution. Thus, the apparent equivalence of the two approaches for the description of the glass transition lies in the fact that any change will influence both the intra- and intermolecular contributions to the overall potential. Therefore, different factors imposed during curing (e.g. heating procedure, time and frequency of mechanical stirring and sonication) and the incorporation of fillers and/or small molecules, such as water, strongly affect the dynamic mechanical behaviour.

### 3.2. Sub-cured DGEBA/TETA/CB composites

The typical DMA traces of dynamic storage modulus ($E'$) and loss tangent tan$\delta$ for the unfilled resin and the DGEBA/TETA/CB system cured at 60°C for 20 hours (sub-curing) are respectively presented in Figures 1 and 2.

An anisotropic behaviour of modulus $E'$ is clearly detected, as it is strongly affected by the filler content in the glassy state and slightly in the rubbery one. However, apart from the discontinuity observed for the 0.5% CB loaded sample, the modulus at room temperature interestingly reaches its maximum for 0.7% of CB loading, which is in accordance with the dielectric measurements where the percolation threshold for the same system was observed with 1.0% CB loading [8]. Concerning the dependence of $T_g$ on the filler content, when estimated at the tan$\delta$ maximum, an increase is observed up to a maximum (156°C) corresponding to CB loading of about 0.7%. Therefore we assume that for this filler concentration the crosslink density reaches its maximum value. Beyond this critical concentration $T_g$ is decreasing as at high CB concentration the nanoparticles aggregate [8, 9], yielding the increase of the free volume.

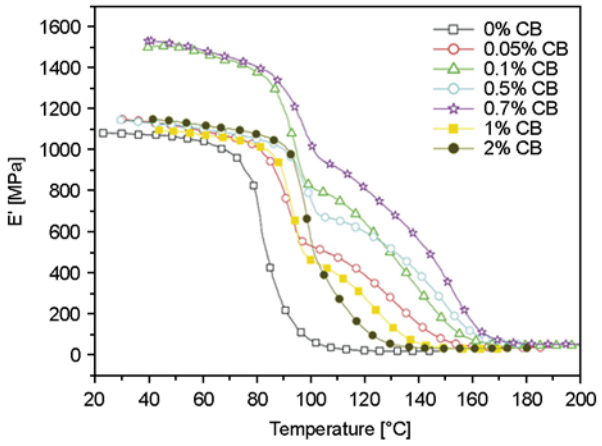


**Figure 1.** $E'$ spectra of DGEBA/TETA/CB with temperature. Curing conditions: 60°C for 20 hours (sub-cured).

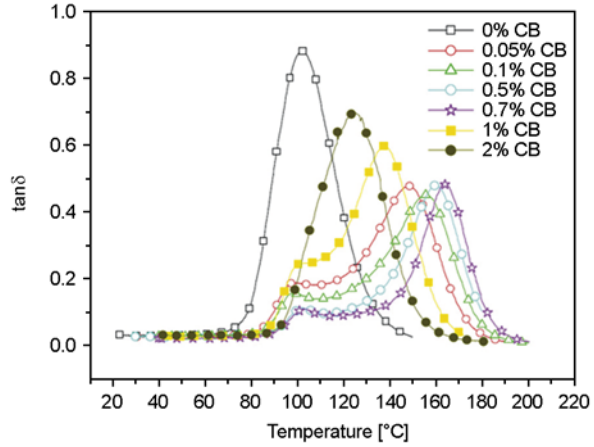


**Figure 2.** Tan$\delta$ spectra of DGEBA/TETA/CB with temperature. Curing conditions: 60°C for 20 hours (sub-cured).

The height and width of the peaks in tanδ spectra provide additional information about the relaxation behaviour of these samples. The height of the peak for the neat resin has a value 0.9, while for the composites it varies between 0.4–0.7 respectively for 0.7–2% CB loading. This implies that the composites exhibit more elastic behaviour than the neat resin. The significant change in the width of the peak suggests a broader distribution of relaxation times, presumably due to more nanoparticle-polymer interactions, and hence restricted mobility.

In addition to this, a new relaxation peak is observed just below the $T_g$ in the partially cured nanocomposites, at the same temperature as for the pure resin. This indicates, at a first glance, the existence of at least two underlying mechanisms of α-relaxation in these curing stages. The first mechanism is caused by the reaction of the crosslink agent with the epoxy groups giving rise to the dominant α-relaxation, while the second one appears as a result of the filler's effect on the curing reaction. The formation of a few nanometres thick intermediate layer on the resin-filler interface, as it has already been reported in [4, 5, 11, 22], probably occurs before the full cure of the composite, thereby inducing the growth of the secondary peak demonstrated in Figure 2. However, as the crosslink density increases in the post-cured composites, the interface region is significantly reduced and the sub-$T_g$ relaxations disappear due to the final incorporation of the loose chains into the main network.

### 3.3. DGEBA/TETA/MWCNT water saturated composites

The DMA spectra of storage modulus $E'$ and tan$\delta$ for the water saturated samples of the DGEBA/TETA/MWCNTs composites are depicted in Figures 3 and 4. It is hence clearly seen that an additional relaxation peak occurs below $T_g$, at the same temperature as for the transition of the pure resin. These spectra are quite similar to those observed in sub-cured epoxy composites filled with CB (Figures 1 and 2).

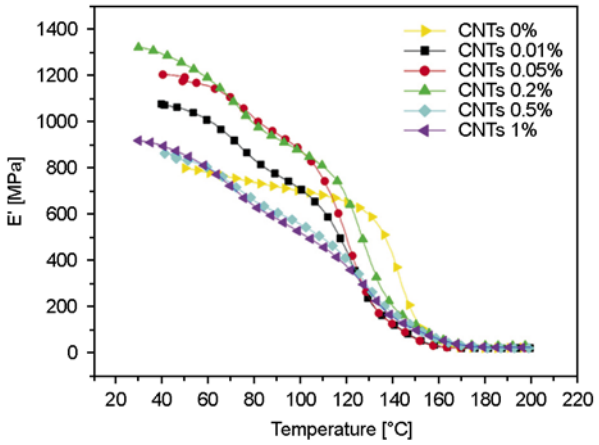


**Figure 3.** $E'$ spectra of water saturated DGEBA/TETA/MWCNTs composites with temperature. Curing conditions: 60°C for 20 hours (sub-cured) and 150°C for 2 hours (post-cured).

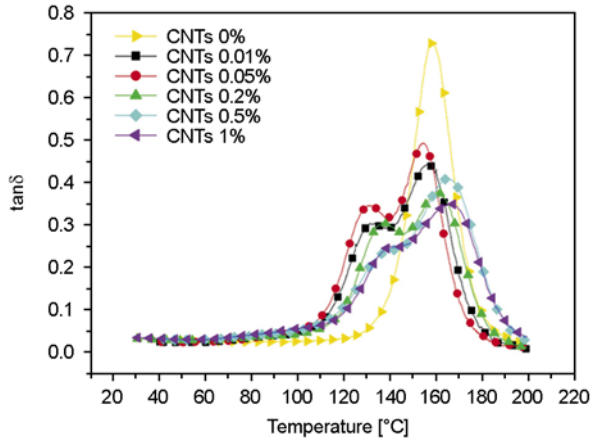


**Figure 4.** Tan $\delta$ spectra of water saturated DGEBA/TETA/MWCNTs composites with temperature. Curing conditions: 60°C for 20 hours (sub-cured) and 150°C for 2 hours (post-cured).

The obtained values of the main and sub-$T_g$ temperature for the case of 0.05% CNT content are displayed in Figure 5. This extra relaxation peak is attributed to the bound water molecules either acting as a plasticizer or participating in the network via hydrogen bonding [14, 23]. Thus, by affecting

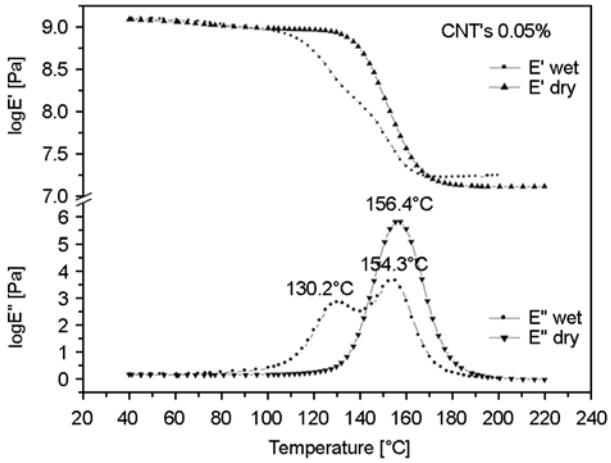


**Figure 5.** $E'$ and $E''$ spectra of DGEBA/TETA/MWCNTs with 0.05% filler content, wet and dried at 220°C

the inter- and intra-molecular flexibility of the backbone it introduces a new relaxation mechanism. In fact, the absence of any sub-$T_g$ relaxation in the unfilled resin (Figure 4) along with its disappearance after the water removal, which is noticed in Figure 5, bear additional evidence of this process.

### 3.4. $T_g$ calculation and network homogeneity

According to the computational process described in Section 2.3, the broad α-relaxation peak is considered as the master curve of the multiple $\alpha_i$-rexations, each with a different sub-glass transition temperature $T_i$. Thereby, the analyzed tan $\delta$ curves for samples with 0.1 and 0.7% CB content are shown in Figures 6a and 6b. In both spectra the experimental peak is reconstructed by six smaller, namely the dominant one close to the experimental maximum, four peaks at lower temperature and a small one at higher temperature. By using the optimization algorithm the characteristic maximum temperature $T_i$ and the full width at half maximum $H_i$ of the sub-$\alpha_i$-relaxations were obtained, whereas the bounded area $S_i$ was calculated from Equation (5). The results

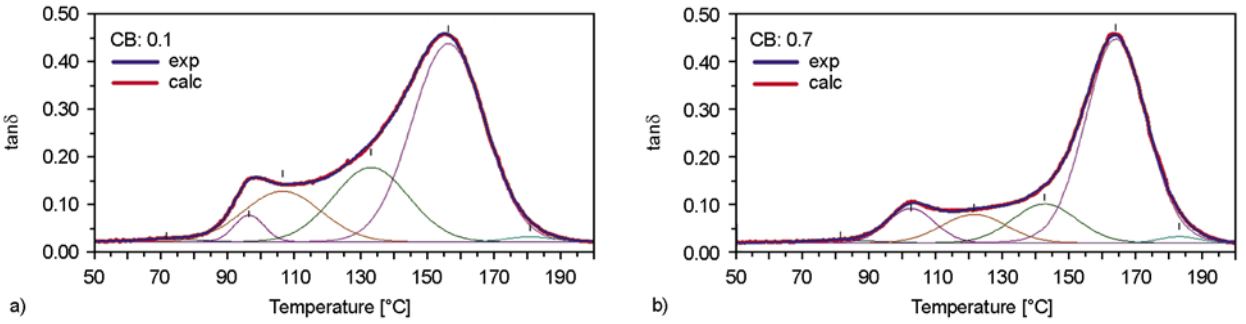


**Figure 6.** Computational analysis of tanδ curves for DGEBA/TETA/CB with a) 0.1% and b) 0.7% CB

**Table 1.** Computational analysis results for DGEBA/TETA/CB with 0.1% CB

| Curve | $T_i$ [°C] | $y_i$ | $H_i$ [°C] | $S_i$ |
|---|---|---|---|---|
| 1 | 72 | 0.006 | 21.968 | 0.136 |
| 2 | 97 | 0.056 | 10.478 | 0.627 |
| 3 | 107 | 0.106 | 27.335 | 3.099 |
| 4 | 133 | 0.156 | 26.659 | 4.451 |
| 5 | 156 | 0.416 | 25.723 | 11.437 |
| 6 | 181 | 0.010 | 16.786 | 0.184 |

for the composite with 0.1% CB content are presented in Table 1.

The contribution weight of each sub-relaxation to the formation of the master curve depends on its characteristics. Taking this into account, the calculated glass transition ($T_{gc}$) can be introduced by Equation (6):

$$T_{gc} = \frac{\sum T_i \cdot S_i}{\sum S_i} \quad (6)$$

A comparison between the calculated $T_{gc}$ from Equation (6) and the estimated values of $T_{g\,exp}$ from the tan $\delta$ maximum is provided in Table 2 for different CB loadings. These new $T_{g\,c}$ values are up to 9% lower than the experimentally estimated values $T_{g\,exp}$. However, they should be more reliable in describing the α-relaxation with a complex profile, since they solely reflect the phenomenon under test, contrary to $T_{g\,exp}$.

Similarly, the analysis of the tan $\delta$ curves of the samples with 0.05 and 0.20% CNT content is depicted in Figures 7a and 7b, where both spectra appear to comprise four different peaks. The obtained characteristic parameters for the DGEBA/TETA/MWCNTs composites with 0.05% nanotubes content are listed in Table 3. The corresponding $T_{g\,c}$ values are calculated from Equation (6) and presented in Table 4, in addition to the estimated $T_{g\,exp}$. These new $T_{g\,c}$ values are again up to 7% lower than the initially estimated from the tan $\delta$ maximum. Moreover, it is evident that the two main peaks are comparable concerning their height and the included area. This indicates the existence of basically two mechanisms with similar characteristics, responsible for the formation of the peak in tan $\delta$ spectra.

The network architecture is a key issue in the analysis of complex α-relaxation in polymer composites. In a 'perfect' network the α-relaxation peak is expected to possess a Gaussian bell-shaped distribution. In any other case the deviation from the Gaussian behaviour can be considered as an evidence of heterogeneity and lack of cohesion of the

**Table 3.** Computational analysis results for DGEBA/TETA/MWCNTs with 0.05% of CNTs

| Curve | $T_i$ [°C] | $y_i$ | $H_i$ [°C] | $S_i$ |
|---|---|---|---|---|
| 1 | 106 | 0.018 | 27.482 | 0.531 |
| 2 | 131 | 0.310 | 24.020 | 8.035 |
| 3 | 155 | 0.442 | 18.799 | 8.965 |
| 4 | 173 | 0.033 | 19.021 | 0.673 |

**Table 2.** Comparison between experimental ($T_{g\,exp}$) and calculated ($T_{g\,c}$) values for DGEBA/TETA/CB with different CB contents

| CB % | $T_{g\,exp}$ [°C] | $T_{g\,c}$ [°C] | $T_{g\,exp} - T_{g\,c}$ [°C] |
|---|---|---|---|
| 0.05 | 148 | 135 | 13 |
| 0.1 | 155 | 141 | 14 |
| 0.5 | 160 | 148 | 12 |
| 0.7 | 164 | 151 | 12 |
| 1.0 | 137 | 130 | 8 |
| 2.0 | 124 | 121 | 3 |

**Table 4.** Comparison between experimental ($T_{g\,exp}$) and calculated ($T_{g\,c}$) values for DGEBA/TETA/MWCNTs with different CNTs contents

| CNTs % | $T_{g\,exp}$ [°C] | $T_{g\,c}$ [°C] | $T_{g\,exp} - T_{g\,c}$ [°C] |
|---|---|---|---|
| 0.01 | 157 | 152 | 5 |
| 0.05 | 155 | 144 | 11 |
| 0.2 | 161 | 150 | 11 |
| 0.3 | 159 | 150 | 9 |
| 0.5 | 165 | 155 | 10 |
| 1 | 167 | 155 | 12 |

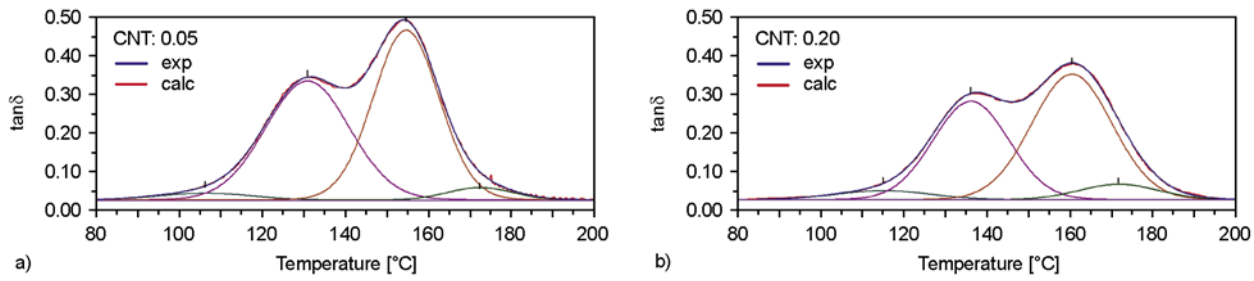


**Figure 7.** Computational analysis of tan $\delta$ curves for DGEBA/TETA/MWCNTs with a) 0.05% and b) 0.2% CNTs.

network due to various phenomena, such as entanglements, free chain ends and complexities produced by the incorporation of the nanoparticles into the backbone of the network. In order to quantify this deviation, based on the above described computational analysis we introduce an index for the network homogeneity (*IH*), calculated from Equation (7):

$$IH = \frac{S_{\mathrm{KDom}}}{S_{\mathrm{KDom}} + \sum_{i=1}^{n} S_{\mathrm{Ki}}} \tag{7}$$

where $S_{\mathrm{KDom}}$ is the bounded area of the main peak and $S_{\mathrm{Ki}}$ corresponds to the ith secondary peak. For the post-cured pure epoxy matrix the Equation (7) yields the *IH* value 0.92. Although, *IH* and $T_g$ are influenced by the nanoparticles loading on the basis of the same phenomena, they are not by definition proportional to each other. Moreover, on the strength of the Equation (7), we deduce that *IH* may theoretically range up to 1.

Based on these remarks, the calculated values of *IH* for various composites containing CB are shown in Figure 8. It can be derived that the *IH* of the nanocomposites is highly dependent on CB concentration. Specifically, there is an initial increase of *IH* up to a definite maximum of about 0.66 for 0.7% CB content, whereas it decreases for higher filler content. Taking into consideration the occurrence of the percolation threshold at 1.0% CB loading [8], the decrease of the main peak contribution and thus of *IH* for loading above that value may be ascribed to the increase of the network agglomerations and inhomogeneities. Besides, a variety of network

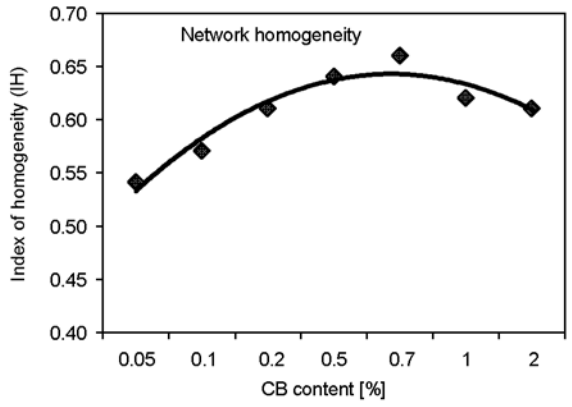


**Figure 8.** The index of network homogeneity *IH* as a function of CB nanoparticles content in sub-cured epoxy composites

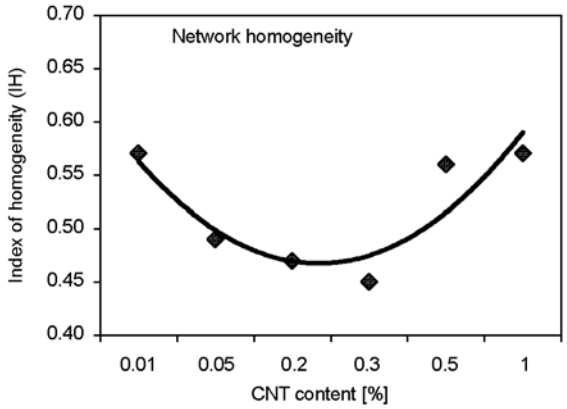


**Figure 9.** The index of network homogeneity *IH* as a function of MWCNTs content in epoxy composites

defects, such as dangling ends, elastically ineffective loops and entanglements, are known to occur in the epoxy-filler system, liberating an increased number of interaction sites or crosslinking species.

In contrast with the dependence of the index *IH* on the CB content, the reverse variation of *IH* is observed in water saturated composites with MWCNTs. The estimated *IH* values for water saturated composites containing MWCNTs as a function of filler content are shown in Figure 9. The drawn data reveal the decrease in IH from 0.57 to a minimum of 0.45 for 0.3% CNTs content, followed by an increase for higher loading. Since the water uptake is related to the small network homogeneity, this trend may reflect the initial increase of the absorbed water. Furthermore, for 0.5–1% CNT concentration the absorption level diminishes to that of the pure epoxy [24], which may also account for the steady *IH* values of the highly loaded samples. Generally, *IH* of the CNT composites are lower than those of the CB sub-cured composites, which can be attributed to the water uptake that alters the network response to the mechanical perturbations. This assumption is further supported by the diagrams of Figures 7a and 7b, where the appearance of two major peaks with comparable size indicates the evenly strong contribution of the water-related relaxation.

## 4. Conclusions

In this research the complex relaxation spectra obtained from the thermomechanical characterization of epoxy nanocomposites are analyzed into their constituent curves corresponding to individual relaxation mechanisms. A computational method is

employed for the extraction of useful information about the mechanisms responsible for the α-relaxation in polymer composites. This analysis is based on the analogy between the bounded area by the curves and the respective relaxation strength. In this framework, two systems of epoxy nanocomposites are studied, namely the subcured DGEBA/TETA/CB and the water saturated DGEBA/TETA/MWCNTs, for which the complex α-relaxation spectra possibly occur due to the formation of two separate coexisting networks. This refers to the network of the pure epoxy matrix and the network formed by the nanoparticles either through the filler-epoxy interface (CB) or through the participation of the amino functionalized CNTs to the crosslinking procedure (MWCNTs). The correspondence of the calculated constituent peaks with the respective network is supported by experimental findings. Furthermore, our technique enables the more precise description of the α-relaxation and the evaluation of the actual $T_g$. Finally, the network complexity due to various defects seems to be related to the α-relaxation profile. Therefore, the analysis of the relaxation spectrum with the assistance of the introduced index *IH* can be used for the qualitative and quantitative assessment of any composite system's homogeneity. The variation in the calculated homogeneity of the two investigated systems is in agreement with the occurrence of network defects above the percolation threshold and the increase of the water content.

## Acknowledgements

Acknowledgements are expressed to Professor P. Pissis for the stimulating discussions during this work and to students Eleni Nikolaidou and Christos Liakopoulos for their contribution to sample preparation.

## References

[1] Dresselhaus M. S., Dresselhaus G., Avouris P., Smalley R. E.: Carbon nanotubes, synthesis, structure, properties and applications. Springer-Verlag, Berlin (2001).

[2] Mai Y., Yu Z.: Polymer nanocomposites, CRC Press, Boca Raton (2006).

[3] Karippal J. J., Narasimha Murthy H. N., Rai K. S., Krishna M., Sreejith M.: The processing and characterization of MWCNT/epoxy and CB/epoxy nanocomposites using twin screw extrusion. Polymer-Plastics Technology Engineering, **49**, 1207–1213 (2010). DOI: 10.1080/03602559.2010.496413

[4] Hergeth W-D., Steinau U-J., Bittrich H-J., Simon G., Schmutzler K.: Polymerization in the presence of seeds. Part IV: Emulsion polymers containing inorganic filler particles. Polymer, **30**, 254–258 (1989). DOI: 10.1016/0032-3861(89)90114-6

[5] Kotsilkova R., Fragiadakis D., Pissis P.: Reinforcement effect of carbon nanofillers in an epoxy resin system: Rheology, molecular dynamics, and mechanical studies. Journal of Polymer Science Part B: Polymer Physics, **43**, 522–533 (2005). DOI: 10.1002/polb.20352

[6] Ash B. J., Schadler L. S., Siegel R. W.: Glass transition behavior of alumina/polymethylmethacrylate nanocomposites. Materials Letters, **55**, 83–87 (2002). DOI: 10.1016/S0167-577X(01)00626-7

[7] Shen J., Huang W., Wu L., Hu Y., Ye M.: The reinforcement role of different amino-functionalized multiwalled carbon nanotubes in epoxy nanocomposites. Composites Science and Technology, **67**, 3041–3050 (2007). DOI: 10.1016/j.compscitech.2007.04.025

[8] Kosmidou T. V., Vatalis A. S., Delides C. G., Logakis E., Pissis P., Papanicolaou G. C.: Structural, mechanical and electrical characterization of epoxy-amine/carbon black nanocomposites. Express Polymer Letters, **2**, 364–372 (2008). DOI: 10.3144/expresspolymlett.2008.43

[9] Brown J., Rhoney I., Pethrick R. A.: Epoxy resin based nanocomposites: 1. Diglycidylether of bisphenol A (DGEBA) with triethylenetetramine (TETA). Polymer International, **53**, 2130–2137 (2004). DOI: 10.1002/pi.1638

[10] Allaoui A., El Bounia N.: How carbon nanotubes affect the cure kinetics and glass transition temperature of their epoxy composites? – A review. Express Polymer Letters, **3**, 588–594 (2009). DOI: 10.3144/expresspolymlett.2009.73

[11] Sun Y., Zhang Z., Moon K-S., Wong C. P.: Glass transition and relaxation behavior of epoxy nanocomposites. Journal of Polymer Science Part B: Polymer Physics, **42**, 3849–3858 (2004). DOI: 10.1002/polb.20251

[12] Hemmati M., Rahimi G. H., Kaganj A. B., Sepehri S., Rashidi A. M.: Rheological and mechanical characterization of multi-walled carbon nanotubes/polypropylene nanocomposites. Journal of Macromolecular Science Part B, **47**, 1176–1187 (2008). DOI: 10.1080/00222340802403396

[13] Prashantha K., Soulestin J., Lacrampe M. F., Claes M., Dupin G., Krawczak P.: Multi-walled carbon nanotube filled polypropylene nanocomposites based on masterbatch route: Improvement of dispersion and mechanical properties through PP-g-MA addition. Express Polymer Letters, **2**, 735–745 (2008). DOI: 10.3144/expresspolymlett.2008.87

[14] Papanicolaou G. C., Kosmidou T. V., Vatalis A. S., Delides C. G.: Water absorption mechanism and some anomalous effects on the mechanical and viscoelastic behavior of an epoxy system. Journal of Applied Polymer Science, **99**, 1328–1339 (2006).
DOI: 10.1002/app.22095

[15] Pethrick R. A., Amornsaichai T., North A. M.: Introduction to molecular motion in polymers. Whittles Publishing, Dunbeath (2011).

[16] Lakes R. S.: Viscoelastic solids. CRC Press, Boca Raton (1998).

[17] Liu Y., Wang Y-F., Gerasimov T. G., Heffner K. H., Harmon J. P.: Thermal analysis of novel underfill materials with optimum processing characteristics. Journal of Applied Polymer Science, **98**, 1300–1307 (2005).
DOI: 10.1002/app.22272

[18] Psarras G. C., Gatos K. G., Karahaliou P. K., Georga S. N., Krontiras C. A., Karger-Kocsis J.: Relaxation phenomena in rubber/layered silicate nanocomposites. Express Polymer Letters, **1**, 837–845 (2007).
DOI: 10.3144/expresspolymlett.2007.116

[19] Becker O., Simon G. P., Dusek K.: Epoxy layered silicate nanocomposites. Advance Polymer Science, **179**, 329–347 (2005).
DOI: 10.1007/b107204

[20] Komorida Y., Mito M., Deguchi H., Takagi S., Millán A., Silva N. J. O., Palacio F.: Surface and core magnetic anisotropy in maghemite nanoparticles determined by pressure experiments. Applied Physics Letters, **94**, 202503/1–202503/3 (2009).
DOI: 10.1063/1.3131782

[21] Zhang L., Yilmaz E. D., Schjødt-Thomsen J., Rauhe J. C. M., Pyrz R.: MWNT reinforced polyurethane foam: Processing, characterization and modelling of mechanical properties. Composites Science and Technology, **71**, 877–884 (2011).
DOI: 10.1016/j.compscitech.2011.02.002

[22] Li B., Zhong W-H.: Review on polymer/graphite nanoplatelet nanocomposites. Journal of Materials Science, **46**, 5595–5614 (2011).
DOI: 10.1007/s10853-011-5572-y

[23] Zhou J., Lucas J. P.: Hygrothermal effects of epoxy resin. Part I: the nature of water in epoxy. Polymer, **40**, 5505–5512 (1999).
DOI: 10.1016/S0032-3861(98)00790-3

[24] Sanchez-Garcia M. D., Lagaron J. M., Hoa S. V.: Effect of addition of carbon nanofibers and carbon nanotubes on properties of thermoplastic biopolymers. Composites Science and Technology, **70**, 1095–1105 (2010).
DOI: 10.1016/j.compscitech.2010.02.015